NIH Public Access
Author Manuscript
Transl Stroke Res. Author manuscript; available in PMC 2014 April 01.

Published in final edited form as:
Transl Stroke Res. 2013 April 1; 4(2): 158–170. doi:10.1007/s12975-012-0213-6.

Vascular endothelial growth factors A and C are induced in the SVZ following neonatal hypoxia-ischemia and exert different effects on neonatal glial progenitors

Jennifer M. Bain, MD PhD[1,2,3], **Lisamarie Moore, MS**[1,2,3], **Zhihua Ren, MD PhD**[1,2,3], **Sophia Simonishvili, PhD**[1,2,3], and **Steven W. Levison, PhD**[1,2,3]

[1]UMDNJ – New Jersey Medical School, Department of Neurology & Neurosciences, University Hospital Cancer Center, Newark, NJ 07103

[2]UMDNJ - Graduate School Biomedical Sciences, University Hospital Cancer Center, Newark, NJ 07103

[3]New Jersey Medical School University Hospital Cancer Center, Newark, NJ 07103

Abstract

Episodes of neonatal hypoxia-ischemia (H-I) are strongly associated with cerebral palsy and a wide spectrum of other neurological deficits in children. Two key processes required to repair damaged organs are to amplify the number of precursors capable of regenerating damaged cells and to direct their differentiation towards the cell types that need to be replaced. Since hypoxia induces vascular endothelial growth factor (VEGF) production, it is logical to predict that VEGFs are key mediators of tissue repair after H-I injury. The goal of this study was to test the hypothesis that certain VEGF isoforms increase during recovery from neonatal H-I and that they would differentially affect the proliferation and differentiation of subventricular zone (SVZ) progenitors. During the acute recovery period from H-I both VEGF-A and VEGF-C were transiently induced in the SVZ, which correlated with an increase in SVZ blood vessel diameter. These growth factors were produced by glial progenitors, astrocytes and to a lesser extent, microglia. VEGF-A promoted the production of astrocytes from SVZ glial progenitors while VEGF-C stimulated the proliferation of both early and late oligodendrocyte progenitors, which was abolished by blocking the VEGFR-3. Altogether, these results provide new insights into the signals that coordinate the reactive responses of the progenitors in the SVZ to neonatal H-I. Our studies further suggest that therapeutics that extend VEGF-C production and/or agonists that stimulate the VEGFR-3 will promote oligodendrocyte progenitor cell development to enhance myelination after perinatal brain injury.

Introduction

The subventricular zone, (SVZ) a remnant of the embryonic germinal zones, is a heterogeneous cellular population, consisting of neural stem cells and progenitors of various potentialities. In the neonatal period, which is when large numbers of glial cells are being generated, the SVZ contains large numbers of bipotential and multipotential glial progenitors that produce immature astrocytes and oligodendrocyte progenitors (OPCs).

Correspondence to: Steven W. Levison, Professor of Neuroscience, Co-Director, Integrative Neuroscience Graduate Program, Director, Laboratory for Regenerative Neurobiology, Department of Neurology and Neurosciences and NJMS-UH Cancer Center, Office H-1226, 205 South Orange Ave, Newark, NJ 07103, PH (973) 972-5162, Fax (973) 972-2668.

Conflict of Interest Statement:
The authors declare that they have no conflict of interest.

NIH-PA Author Manuscript
NIH-PA Author Manuscript
NIH-PA Author Manuscript

NIH-PA Author Manuscript

NIH-PA Author Manuscript

NIH-PA Author Manuscript

These glial precursors migrate from the SVZ laterally to adjacent striatum, dorsally to the white matter and the neocortical gray matter, giving rise to astrocytes, oligodendrocytes and polydendrocytes (1). The differentiation of a bipotential glial progenitor into either an astrocyte or an oligodendrocyte is regulated by complex interaction of extrinsic and intrinsic cues. A fundamental question that remains unanswered is what are the extrinsic signals that affect the specification of the neural stem cells and progenitor cells of the SVZ during development and also after injury?

Hypoxia-ischemia (H-I) is a condition in which there is both lack of blood flow and low oxygen tension in the brain leading to some degree of neurological deficit. Infants who survive episodes of H-I may develop cerebral palsy, epilepsy, developmental disabilities or hypoxic-ischemic encephalopathy (HIE), a commonly used catch-all phrase describing the nonspecific clinical picture after neonatal H-I. H-I is regarded as the major cause of brain damage in the term infant (2–4). The pathophysiology of H-I involves ATP depletion, excitotoxicity, calcium toxicity, and free radical damage; however inflammation also plays a significant role, contributing to both apoptosis and necrosis of many cells, notably the neurons and oligodendrocyte progenitors (5–11). The particular depletion of oligodendrocyte progenitors in the white matter presents a major problem because neurogenesis is not sufficient without concurrent gliogenesis to restore functional recovery after injury (12–14).

Studies in the adult brain after hypoxia show that the vascular endothelial growth factors (VEGF) and their corresponding receptors participate in hypoxia-induced neovascularization. Hypoxia-inducible Factor-1 (HIF-1) is a classic activator of VEGF production; however other studies suggest roles for glucose deprivation, platelet-derived growth factor (PDGF), IL-1β, TGFβ1 and tumor necrosis factor-alpha (TNF-α) (15). There are 7 members of the VEGF family, A, B, C, D and placenta-derived growth factor, which bind to the tyrosine kinase receptors VEGFR-1 (Flt-1), VEGFR-2 (Flk-1 or KDR), VEGFR-3 (Flt-4), to neuropilins-1 and -2 and to heparin sulfate proteoglycans (15). While all of the VEGF isoforms regulate angiogenesis, recent evidence suggests that some isoforms promote proliferation of other cells types. Studies show that VEGF-A stimulates the proliferation of astrocytes, Schwann cells, microglia and cortical neuroblasts, as well as the proliferation, migration and survival of neural stem cells in the SVZ, subgranular zone of the hippocampal dentate gyrus and olfactory bulb (15–23). Interestingly, Mani et al. 2005 showed that administrating VEGF-A to embryonic and adult rat neocortical explant cultures significantly increased the entire astroglial profile by increasing the percentage of mature GFAP+ cells, as well as immature nestin+ and vimentin+ cells via the Flt-1 receptor (24). Whereas there have been several studies examining the effects of VEGF-A on CNS cells, there are few studies examining VEGF-C. One study conducted on VEGF-C deficient mouse embryos showed selective loss of oligodendrocyte progenitors cells (OPCs). Furthermore, VEGF-C induced optic nerve OPCs to proliferate, while VEGF-A did not induce BrdU incorporation (25). Given that there is an aberrant production of astrocytes from SVZ precursors after H-I, we hypothesized that amongst the VEGFs, that VEGF-A might be uniquely produced in the SVZ after neonatal H-I. Furthermore, we sought to better characterize the effects of VEGF-C on different progenitor populations, specifically via the VEGFR-3 receptor.

Materials and Methods

Neonatal Hypoxia/Ischemia

All experiments were performed in accordance with research guidelines set forth by the New Jersey Medical School and the Society for Neuroscience Policy on the use of animals in neuroscience research. Cerebral H-I was induced in P6 rats (day of birth being P0), by a

NIH-PA Author Manuscript

NIH-PA Author Manuscript

NIH-PA Author Manuscript

permanent unilateral (right) common carotid artery cauterization under isoflurane anesthesia followed by systemic hypoxia (26–28). The neck wound was sutured with surgical silk and the animals were returned to the dam to recover for 1.5 h. Animals were then pre-warmed in jars for 20 min in a 37°C water bath. The pups were exposed to a humidified, hypoxic atmosphere (8% O_2/92% N_2) at 37°C for 70 min, allowed to recover in room air, and then returned to their dams. Control animals were separated from the dam for the same amount of time as experimental animals, but were otherwise untouched.

ELISA

Tissue was isolated from microdissected SVZs and protein extracted in lysis buffer (ice cold phosphate buffered saline with 1% Triton-X-100, 0.1% SDS, 1% protease inhibitor cocktail (Sigma P8340), 1% Na_3VO_4, 1% PMSF (phenylmethylsulphonyl fluoride), 1% NaF) followed by sonication and centrifugation. Matched antibody pairs for sandwich ELISAs from R&D for rat VEGF-A (monoclonal anti-rat VEGF-Antibody (MAB564) and biotinylated anti-rat VEGF-Antibody (BAF564)) and human VEGF-C (monoclonal anti-human VEGF-C antibody (MAB752) and biotinylated anti-human VEGF-C antibody (BAF752)) were used on 10 μg of protein samples isolated from microdissected SVZs at various time points after injury. ELISAs were also used to determine protein concentrations of supernatants (100 μL) from spheroids, astrocytes and microglia cultures placed under control or hypoxic-glucopenic (HG) (2% O_2) for 2 h and supernatant collected after 18 h (see section “Microglia, astrocyte and oligodendrocyte progenitor cultures” for more information).

Western Blot

Neurospheres, spheroids, OPCs and astrocyte cultures were generated from neonatal rat brains using standard methods, as described in later methods sections. Cells were collected by centrifugation and lysed with 1% Triton-X, 0.1% SDS, 1% 0.1M sodium orthovanadate and protease inhibitor cocktail (Roche Diagnostics) dissolved in PBS. The cells were sonicated then centrifuged at 10,000 rpm for 15 minutes at 4°C. The protein concentration was quantified with the Pierce BCA Protein Assay Kit (ThermoScientific). Thirty μg of denatured protein was loaded onto a 4–12% Novex NuPage Bis Tris Gel (Invitrogen) then transferred to nitrocellulose (Invitrogen). Blots were probed with rabbit anti-VEGFR-3 (1:100 Santa Cruz), mouse anti-βactin (1:5000, Sigma-Aldrich), washed and incubated with secondary antibody against rabbit or mouse conjugated to HRP (1:2500, Jackson ImmunoResearch Laboratories). Signals were detected by chemiluminescence-ECL (PerkinElmer) and quantified using a UVP Bioimaging system.

RNA Isolation, cDNA Reverse Transcriptase Reaction and QRT-PCR

Quantitative real-time PCR was performed on micro-dissected SVZs. mRNAs were extracted from post-H-I rat SVZs at 6, 12 and 24 hours, as well as days 2 and 7 and corresponding cDNA was made using reverse transcription reaction. Custom-designed VEGF primers were optimized for SYBR Green chemistry and analyzed using an Applied Biosystems 7300 Real-Time PCR System Sequence Detection Systems v.1.2.3 (Foster City, CA) (Table 1). The ipsilateral (IL) hemisphere was compared to contralateral (CL) hemisphere and non-hypoxic control hemispheres. Applied Biosystems SDS 2.2.2 relative quantification (ΔΔCt) assay was used to quantify mRNA expression and results are presented as RQ values.

Tissue Fixation and Histochemistry

Experimental animals were anesthetized with a mixture of ketamine (75 mg/kg) and xylazine (5 mg/kg) prior to perfusion with RPMI culture medium containing 6 units/ml

NIH-PA Author Manuscript

NIH-PA Author Manuscript

NIH-PA Author Manuscript

heparin followed by 4% paraformaldehyde (PFA) in 0.1 M phosphate buffer, pH 7.4. The brains were removed and immediately transferred to 4% PFA overnight at 4° C. Brains were transferred to a 30% sucrose solution for 24 h at 4°C followed by 4 h with fresh 30% sucrose solution before being fixed frozen on a dry ice-ethanol slush in embedding medium and stored at −80°C.

Microvascular Luminal Areas

To quantify the luminal areas of SVZ microvessels, sections at recovery times spanning 4 to 48 h after H-I were stained with hematoxylin and eosin. Blood vessels were identified by morphology and chosen at random. Luminal areas were measured using IP Lab software (Scanalytics, Inc. Fairfax, Virginia USA) on 40X images. The sections from 4 h brains were stained for BrdU, tomato lectin and DAPI to label proliferating blood vessel endothelial cells in hemispheres of H-I and non-hypoxic controls. Corresponding vessels were measured from 3 random, nonadjacent SVZ sections and 4 animals at each time point.

Neurosphere and spheroid cell cultures

P4 rat pups were decapitated under sterile conditions and the brains were placed into phosphate buffered saline (PBS) with 0.6% glucose and 2 mM $MgCl_2$. Incisions were made ~2 mm from the anterior end of the brain and ~3 mm posterior to the first cut. Blocks were transferred to fresh PBS-glucose-$MgCl_2$. The region including the SVZ was microsurgically isolated, mechanically minced and enzymatically dissociated using 1:4 dilution of Accutase (Innovative Cell Technologies, CA) @ 37° C for 10 min. Neurospheres were generated using EGF and FGF-2 supplemented medium whereas glial progenitors were propagated as spheroids using medium supplemented with 30% B104 conditioned medium (CM) (29). The ProN base growth medium contained Dulbecco's modified eagle's medium (DMEM)/F12 supplemented with 10ng/ml d-biotin, 25 μg/ml insulin, 20 nM progesterone, 100 μM putrescine, 5ng/ml selenium, 50 μg/ml apo-transferrin and 50 μg/ml gentamycin. Spheroids were generated in a 2% O_2, 5% CO_2, 93% N_2 37°C incubator. To dissociate or passage the spheroids, cells were treated with a pH-balanced enzyme solution containing collagenase III (0.002 g), papain (200U), and DNase I (100uL of 5mg/mL stock) in 10 mL Papain Buffer (DMEM/F12 with 0.48 g HEPES, 0.02 g EDTA and 0.0175 g L-cysteine. Differentiation of spheres was performed after dissociation with/without growth factor treatments in N2B2 media [ProN supplemented with 0.66 mg/mL BSA and 0.5% fetal bovine serum] for 72 h.

Microglia, astrocyte and oligodendrocyte progenitor cultures

Newborn Sprague-Dawley rat forebrain cortices were enzymatically digested with trypsin and DNase I and then mechanically dissociated, prior to plating in MEM containing 10% FBS with antibiotics as previously described (30). The mixed glial cells were grown in T75 flasks until they were confluent (10–14 days). Microglia were separated from the cultures by shaking the flasks on a rotary shaker for 1.5 h at 260 rpm. Followed by an additional 18 h shake oligodendrocyte progenitors cells (OPC) were generated and astrocytes were adherent to the flasks. Astrocytes were suspended using 0.25% trypsin/EDTA and then plate at 2×10^4 cells/mL in untreated 6 well dishes. OPCs were seeded into PDL-coated T75 flasks at a density of $1.5 \times 10^4/cm^2$ in a chemically defined media, N2S, composed of: (1) 66% N2B2 media, (2) 34% B104-CM, (3) 5 ng/mL FGF-2, and (4) 0.5% fetal bovine serum. OPC cultures were amplified 4–10 days and passaged once using papain (29) prior to performing experiments. A greater than 95% purity of Early OPCs (A2B5+/O4−) was consistently achieved with these enrichment and culture conditions with <2% contamination with astrocytes and <0.01% contamination with microglia as previously reported (31). Some Early OPCs were allowed to mature into Late OPCs (O4+/Rmab−) by replacing the N2S with 10 ng/ml FGF-2. For immunocytochemistry experiments, cells were plated at a density of 2.0×10^4 cells/cm^2 onto PDL - coated chamber slides in N2S media. 12 – 15 h after

NIH-PA Author Manuscript

NIH-PA Author Manuscript

NIH-PA Author Manuscript

plating for experiments, OPCs were switched to N1A serum-free media to arrest cells in G0/G1. N1A was identical to the N2B2 media described above, with the exception that the insulin concentration was lowered to 5 ng/mL. Cells were treated in N1A media for 6 h prior to growth factor treatment. The media was then replaced with the appropriate growth factors for 18 h followed by 2 h BrdU pulse.

Immunocytochemistry

For characterization studies, cells were fixed and stained with primary antibodies overnight at 4°C, including mouse IgM antibodies against PSA-NCAM (Millipore, Ma; 1:500), A2B5 (supernatant 1:4), D1.1 (supernatant 1:4), R24 (supernatant 1:4), rabbit antibodies against Dlx2 (Millipore, 1:500), NG2 (generously provided by Bill Stallcup 1:200), Olig2 (Millipore, 1:500), GFAP (Dako, 1:500), and mouse IgG against vimentin (V9 clone, Roche, 1:100). For the clonal analyses, spheroids were propagated and dissociated into single cells. Cells were plated onto PDL-coated chamber slides at 2×10^4 cells/well in 1) N2B2 + 2% serum with 700 CFU/well or 2) ProN/B104 + 2% serum with 50 CFU/well for 1 d. Media was then replaced with N2B2 for 5 days to allow differentiation. After live O4 staining, cells were fixed in 4% PFA and stained for GFP (Aves Lab, 1:2,500) and GFAP. For the differentiation experiments, cells were fed with either with N2B2 media alone or N2B2 supplemented with combinations of recombinant rat $VEGF_{164}$ A (R&D Systems, 8 ng/mL) and recombinant human VEGF-C (Cys156Ser) (R&D Systems, 100 ng/mL). After treatment, the cells were fixed for 10 min in 4% PFA and then incubated for 1 h at RT with primary antibodies described above against GFAP or O4 to identify astrocytes and oligodendrocytes, respectively. The cells were washed and further incubated with fluorochome-labeled secondary antibodies for 1 h at RT.

For double labeling of BrdU and GFAP, O4, or PSA-NCAM, cells were pulsed with 10 μM BrdU for 2 h prior to staining. Fixed cells were pretreated in 2N HCl for 15 min at RT to denature DNA and rinsed with borate buffer (pH 8.5). Cells were incubated for 30 min with 0.1M Tris buffer/0.1% Tritron-X-100 followed by a 20 min incubation with 10% BSA, 10% goat serum in Tris buffer. Cells were incubated in primary antibodies, rinses and then incubated in fluorochome-conjugated secondary antibodies. The cells were counterstained with DAPI for 10 minutes. Stained cells were washed thoroughly and mounted with Gel/Mount (Biomeda, CA) and allowed to dry overnight. Immunoreactive cells were visualized using an Olympus AX70 microscope and images of stained cells were collected using a Photometrics cooled charged coupled device camera (Tucson, AZ) interfaced with IP Lab scientific imaging software (Scanalytics Fairfax, VA).

In all experiments, labeled cells in at least 4 random (nonadjacent) fields were counted per well under a 20× or 40× objective and a total of 4 wells per independent group were evaluated At least 100 cells were counted based on DAPI staining for each experiment.

BrdU Immunohistochemistry

For BrdU labeling experiment, BrdU (Sigma, at 50 mg/kg body weight, 10 mg/mL in 0.007 N NaOH in 0.9% NaCl) was administered intraperitoneal 4 h following H-I. Thirty minutes later, animals were sacrificed by intracardiac perfusion, cryoprotected, frozen and tissue sections encompassing the region of brain subserved by the middle cerebral artery was cut at 12 μm thickness and mounted onto glass slides. Select tissue sections were incubated for 1 h at RT in 2N HCl, extensively rinsed with borate buffer (pH 8.5), and blocked in a solution containing 10% BSA, 10% goat serum in Tris buffer for 1 h. The sections were then incubated with a rat monoclonal anti-BrdU (Accurate Chemical, NY; 1:30) and biotinylated tomato lectin (Vector Laboratories, CA; 1:100) overnight at 4°C. Sections were further

NIH-PA Author Manuscript

NIH-PA Author Manuscript

NIH-PA Author Manuscript

incubated in fluorochome-conjugated secondary antibodies (Jackson Laboratories, PA; 1:200) for 2 h at room temperature. DAPI was used to stain all nuclei.

VEGF Receptor Blocking Studies

Purified early OPCs were starved in N1A medium (5 ng/ml insulin) for 6 hours. OPCs were then incubated with VEGF-C (Cys156Ser) (R&D Systems; 100ng/ml) and blocking antibodies to either VEGFR-1 (cat #AF471, R&D Systems, 5μg/ml), or VEGFR-2 (cat #AF644, R&D Systems, 0.2 μg/ml), or VEGFR-3 (ImClone IMC-3C5, 7.5μg/ml), or N2B2 medium control for 18 h. IMC3C5 is an antagonist antibody for human VEGFR-3 with cross-reactivity to rat VEGFR-3 (ImClone Systems, unpublished data). After treatment, the OPCs were fixed for 10 min in 3% PFA and then incubated with primary antibodies against Ki67 (Vector Laboratories, 1:1000) and A2B5 (supernatant, 1:5) or O4 (supernatant, 1:4) to identify the proliferating oligodendrocyte at both early and late stages, respectively, at 4°C overnight. The OPCs were then rinsed and incubated in fluorochome-conjugated secondary antibodies for 1 hour at RT, and counterstained with DAPI (Sigma, 1:5000) for 10 minutes. After washed, slides were mounted with Gel/Mount (Biomeda, CA) and allowed to dry overnight. An Olympus AX70 microscope was used to collect images of immunopositive cells. In all experiments, labeled cells were counted in at least 6 random (nonadjacent) fields per well under a 20× or 40× objective lens and a total of 4 wells per independent group were evaluated. At least 500 cells were counted from each treatment group.

Statistical analyses

Results from cell culture were analyzed for statistical significance using a student's *t* test or by ANOVA with Fisher's PLSD post-hoc test. Error bars represent SEMs. Comparisons were interpreted as significant when associated with $p<0.05$.

Results

VEGFs are quickly and transiently up-regulated after neonatal H-I in the SVZ

Sandwich ELISA analyses for VEGF-A and VEGF-C proteins demonstrated induction by 12 and 24 h, respectively, compared to non-hypoxic shams and contralateral hemispheres (Figure 1 A, B). However, both proteins quickly returned to baseline levels within 2 days after injury and remained so up to 7 days post-H-I. Neither VEGF-A, VEGF-B nor VEGF-C mRNA levels increased after H-I (data not shown).

To determine which cell types may be responsible for producing VEGFs, we measured levels of VEGF-A and VEGF-C in culture supernatants from highly enriched astrocyte and microglial cultures. Astrocytes constitutively produced large quantities of VEGF-A, whereas the production of VEGF-A by the microglia was below the level of detection (Figure 1). Whereas the microglia did not produce detectable levels of VEGF-A, they did produce VEGF-C, and exposing the microglia to hypoxic-glucopenic (HG) conditions increased their VEGF-C production. HG also tended to increase VEGF-C production by the astrocytes, although the increase was not statistically significant ($p > 0.05$). The supernatant from SVZ-derived spheroids was also analyzed and found to contain very high levels of VEGF-A, as well as some VEGF-C. These progenitors were grown under 2% O_2, to mimic the in vivo niche, and thus were not further subjected to HG conditions.

Effects of VEGFs on glial progenitors in vitro

Several studies have shown that VEGF proteins can stimulate the proliferation of various neural cell types (16, 23, 25). To determine the effects of VEGFs A and C on SVZ glial progenitors, spheroids were generated in ProN/B104 media for 7–10 days in 2% O_2. Spheroid cells were then exposed to recombinant VEGFs A and/or C overnight (18 h) and

NIH-PA Author Manuscript

NIH-PA Author Manuscript

NIH-PA Author Manuscript

then incubated with 10 uM BrdU for 2 h to label cells entering S-phase of mitosis. Spheres were dissociated gently and stained for PSA-NCAM and BrdU. Neither VEGF-A nor VEGF-C independently increased the percentage of PSA-NCAM+/BrdU+ cells. The combination of VEGF-A and C showed a positive trend, which was not statistically significant (data not shown).

To determine how VEGF-A and C affected cell differentiation, spheroids were generated and subsequently dissociated. Cells were differentiated for 3 days on PDL-coated chamber slides. VEGF-A increased the percentage of GFAP+ cells, while VEGF-C increased the percentage of O4+ cells after 3 days of differentiation *in vitro* (Figure 2 A–D). There was a small percentage of cells that remained unlabeled after differentiation.

To determine whether the VEGFs were affecting the differentiation of the spheres or the proliferation of specific precursors, we performed the same 3 day differentiation experiment with a 4 h BrdU pulse prior to fixation and immunocytochemistry. Both VEGF-A and VEGF-C significantly increased BrdU incorporation in spheroids (Figure 2 E). VEGF-A administration increased BrdU incorporation in the GFAP+ population in spheroids, while VEGF-C did not have any significant effect on BrdU incorporation in the GFAP+ cells. On the other hand, only VEGF-C significantly increased BrdU incorporation of the O4+ population, and this effect was dampened by the addition of VEGF-A to the condition. When both VEGFs were added to the cultures, there was still a significant increase in total BrdU incorporation from the control, which was mostly within the GFAP+ cell population.

Effects of VEGFs on neonatal lineage-restricted glial progenitor cells

We were also interested in whether these VEGFs would induce the proliferation of more lineage-restricted glial cell precursors. To address this question, we generated enriched astrocyte and oligodendrocyte progenitor cultures and treated them overnight (18 h) with VEGFs A and/or C followed by a 2 h BrdU dose. In the astrocyte cultures, both VEGF-A and VEGF-C had significant proliferative effects on the GFAP+ cells individually, and the combined treatment revealed an additive proliferative effect (Figure 3 A).

In enriched early OPCs, an overnight treatment with 8 ng/mL of VEGF-A did not affect on BrdU incorporation; however, overnight treatment with 100 ng/mL VEGF-C significantly increased BrdU incorporation, with a robust doubling of cells passing though the S-phase (Figure 3 B). Adding VEGF-A with VEGF-C significantly dampened this proliferative response. These results support the conclusion that VEGF proteins have significant proliferative effects on lineage-restricted cell types isolated from the neonatal rat brain.

Spheroids express higher levels of VEGFR-3 than glial restricted cells

VEGFR-3 is exclusive to VEGF-C signaling compared to VEGFR-2, which can be activated by multiple members of the VEGF ligand family. Since VEGF-C stimulated the proliferation of OPCs and VEGF-C can bind to both VEGFR-2 and R3, we sought to establish whether OPCs expressed the VEGFR-3 and to compare the level of R3 on OPCs versus other neural precursors. Protein samples from neurospheres, spheroids, astrocytes, early OPCs and late OPCs were separated by gel electrophoresis transferred to nitrocellulose and probed for VEGFR-3 by Western blot. Interestingly, the spheroids, which are comprised of tripotential PDGF responsive progenitors (Moore, Bain et al., submitted) expressed the highest levels of VEGFR-3 with the rank order or spheroids > neurospheres > early OPCs > late OPCs > astrocytes. (Figure 4 A).

NIH-PA Author Manuscript

NIH-PA Author Manuscript

NIH-PA Author Manuscript

Neutralizing the VEGFR-3 abolished VEGF-C stimulated oligodendrocyte proliferation

To establish whether the proliferative effects of VEGF-C were indeed conveyed by the VEGFR-3, experiments were conducted using neutralizing antibodies to VEGFR-1, R2 and R3. For these experiments, early OPCs were incubated with either VEGF-C and neutralizing antibodies to VEGFR-1, VEGFR-2 or VEGFR-3. Cell proliferation was evaluated by double immunostaining for Ki67 with either A2B5 or O4 antibody. As expected, VEGF increased the Ki67 index of both early OPCs and also late OPCs and the neutralizing antibody to VEGFR-3 completely blocked the VEGF-C-stimulated OPC proliferation (Figure 4 B–U). In contrast, neutralizing antibodies to VEGFR-1 or R2 did not inhibit VEGF-C function (Figure 4 V,W).

SVZ microvasculature remodeling after injury

Since the levels of these angiogenic growth factors were increased during the acute recovery interval from neonatal H-I, it was of interest to evaluate microvasculature alterations within the SVZ after neonatal H-I. Hematoxylin and eosin staining was performed on sections 4 to 48 h after H-I and measurements were made of the luminal areas of vessels in the SVZ. At 4 h after injury, there were robust increases in the luminal areas of microvessels in the IL SVZ compared to non-hypoxic (74-fold) and CL hemispheres (4-fold), respectively, which remained significantly higher until at least 48 h after injury (Figure 5). As this increase luminal area could either be due to vasodilatory effects hypoxia or to angiogenesis, we administered BrdU at 4 h after H-I and then, performed immunohistochemical staining using tomato lectin and BrdU, Contrary to the hypothesis that the increase in VEGFs would result in increases in angiogenesis, there was no difference in BrdU incorporation into the endothelial cells within the SVZ (data not shown). These data suggest that the increased luminal area observed in the injured SVZ as early as 4 h after injury is not a consequence of angiogenesis, but rather more likely due to vessel dilation.

Discussion

The goal of this study was to determine whether VEGFs A or C participate in the reactive responses of the progenitors in the SVZ to neonatal H-I. We found that 1) both VEGFs A and C, are quickly and transiently induced in the SVZ during recovery from H-I: 2) that glial progenitors, astrocytes and to a lesser extent, microglia, produce these growth factors; 3) VEGFs A and C differentially affect the production of astrocytes and oligodendrocytes from SVZ-derived spheroids; 4) VEGFs A and C stimulate the proliferation of lineage-restricted astrocyte and oligodendrocyte progenitors and 5) VEGF-C exerts its proliferative effects on OPCs via the VEGFR-3 receptor.

A collection of studies in *Cell Stem Cell* highlighted the importance of the neurovascular stem cell niche during development (32–35). The studies independently examined the intimate relationship between the cerebral vasculature and the neural stem and progenitor cell compartments. We were also interested in evaluating the neurovascular niche of the SVZ after neonatal H-I during the period when we have previously observed proliferative changes in the SVZ cells. We found that two angiogenic proteins, VEGFs A and C, are quickly and transiently increased in the SVZ. Attempts to use immunohistochemistry to establish which cells within the neonatal SVZ were producing these cytokines were ambivalent. We used a previously established *in vitro* model for the multipotential progenitor fraction of the neonatal SVZ to determine how VEGFs would affect their proliferation and differentiation (Moore, Bain et al., 2012; *Accepted pending minor revision*. Next, ELISAs for VEGF-A and VEGF-C were used to measure the production of these factors from astrocytes, microglia and spheroids. We found that the spheroids produced large amounts of both proteins. Astrocytes produced both VEGF-A and VEGF-C, and under

NIH-PA Author Manuscript

NIH-PA Author Manuscript

NIH-PA Author Manuscript

HG conditions, there were slight increases in the protein production. Microglia were a source of VEGF-C, which was significantly up-regulated after HG conditions. Unfortunately, we were unable to compare the amounts of proteins produced by each cell type, as we were limited by our culture techniques and unable to normalize the number of cells in a spheroid and the different plating densities of astrocytes and microglia.

In this study, we found that VEGFs A and C had different effects on multipotential progenitors in the spheres versus more mature glial precursors. When applied to the sphere derived cells, neither VEGF-A nor VEGF-C altered the percentage of PSA-NCAM+ cells and they were weak mitogens for these cells, unlike studies of neural stem cells stimulated by VEGF-A (15, 36, 37). However, we did find that VEGF-A promoted astrocyte proliferation, supporting many studies relating VEGF-A signaling via the R2 receptor (Flk-1) to astrogliogenesis and scar formation after brain injury (38–40). Moreover, these studies provide evidence that VEGF-A can also affect the astrocyte generation from the SVZ, nearby the VEGF-producing choroid plexus (37, 41). We also found VEGF-C supported oligodendrocyte production both in spheroid cultures and forebrain OPC cultures, similar to the trophic effects of VEGF on optic nerve OPCs (25). When these growth factors were applied together to enriched astrocyte cultures they exerted additive proliferative effects. By contrast, combined treatment to OPCs actually decreased the stimulatory effect of VEGF-C on oligodendrocyte progenitor proliferation. These effects are most likely due to differential expression of the VEGF receptors on different glial cell types. In this study we did establish that VEGFR-3 is present in the neonatal SVZ. We were unable to obtain comparison levels of R1 or R2 in this study, however this may have clouded our results and conclusions given the cross talk of VEGF-A and -B ligands with both of these receptors.

The vascular cells of the SVZ are appreciated as important components of the stem cell microenvironment. The microvascular system can exert effects on the growth, survival, differentiation, and migration of stem and progenitor cells (18). As we found that two potent growth factors that affect vascular elements are increased in the SVZ as a consequence of injury, we asked whether there were corresponding changes in the cerebrovasculature of the SVZ. At 4 h after injury, we found a significant increase in the luminal diameter of the ipsilateral SVZ microvasculature, compared to both the contralateral and non-hypoxic controls. However, when we looked at bromodeoxyuridine incorporation at this early time point, we did not find any significant changes in the injured SVZ, suggesting that neovasculogenesis is not the cause of the increased luminal area. More likely, other signaling molecules, such as nitric oxide (NO), possibly induced by VEGF proteins, are having effects on smooth muscle cells in the region causing relaxation of the vasculature. These signaling molecules may also play a role in the neural stem cell niche. For example, NO has been found inhibit proliferation of NSCs in the SVZ, as well as promote neuronal differentiation (42, 43). Given that VEGFs A and C are present in the injured SVZ for up to 24 hours after insult, these proteins may play alternative, non-angiogenic roles during recovery.

Glial scarring is a well-characterized consequence of brain injury. In the mature brain, data suggest that the majority of reactive astrocytes arise from existing astrocytes residing in the penumbra of the injury as a consequence of cytokines produced by damaged neurons and reactive microglia (44–46). Histopathologic studies on the brains of infants who have expired from neonatal H-I have shown that there is significant gliosis in affected regions (47). However, in the immature brain where astrocyte genesis is incomplete, this explanation for the origin of reactive astrocytes cannot completely explain their generation. We have found that VEGF-A and VEGF-C can collaborate to stimulate the expansion of SVZ glial progenitors and that they will increase the production of astrocytes both from SVZ multipotential progenitors as well as from immature astrocytes. These studies confirm that

NIH-PA Author Manuscript

NIH-PA Author Manuscript

NIH-PA Author Manuscript

VEGF-A is important for astrogliogenesis, especially after neonatal H-I (16, 39, 40). However, these studies also extend the role of VEGF-A to having specific effects of SVZ progenitors to generating more astrocytes instead of the more developmentally appropriate oligodendrocytes. In a 2010 study in adult rats, VEGFR-3 was noted to be expressed by multiple progenitor cell types in the SVZ after hypoxic injury, including cells positive for PSA-NCAM, nestin and GFAP (48). Moreover, these cells were highly proliferative, suggesting that VEGFR-3 was an important mediator in adult neurogenesis after ischemic stroke.

In our studies, we show that VEGF-C does exert specific effects on oligodendrocytes of the SVZ, extending the studies by Le Bras et al. that VEGF-C, mediated by VEGFR-3, is important for OPC survival and differentiation. Furthermore, we also found R3 to be a crucial mediator in VEGF-C signaling for OPC proliferation and differentiation. By blocking R3 *in vitro,* we abolished the effects of VEGF-C on OPC cultures. On the other hand, the blocking of R1 and R2 did not have the same effect. This important distinction may elucidate other mechanisms that may be occurring after H-I injury in the neonatal brain. These distinctions may eventually be a target for pharmacologic or gene therapy interventions after injury. Altogether, these results provide new evidence for a role for VEGFs in remodeling the SVZ after neonatal injury. In particular, they provide insights into the origins of the reactive astrocytes that appear during recovery from neonatal H-I. Our studies further suggest that therapeutics that can extend VEGF-C expression, or agonists that can stimulate the VEGFR-3 will enhance the production of oligodendrocyte progenitors to promote myelination after perinatal brain injury.

Acknowledgments

The authors thank ImClone Systems/Eli Lilly for providing the neutralizing antibody to VEGFR-3 (IMC-3C5) and for advice on our studies. We are also grateful to Qasim Husain for assistance with the initial sphere studies and to Kedar Mahajan and Jungsoo Min in Dr. Terri Wood's lab for occasionally providing OPCs from mixed glial cell cultures.

Support: National Institute of Neurological Disorders and Stroke and National Institute of Child Health and Development; Grant Numbers: F31NS062629 awarded to JMB, F31NS076269 awarded to LM, a grant from the Leducq Foundation and R01HD052064 awarded to SWL.

References

1. Levison, SW.; DeVellis, J.; Goldman, JE. Astrocyte Development. In: Jacobsen, MSRaM, editor. Developmental Neurobiology. 4 ed.. New York: Plenum; 2005. p. 197-222.
2. Back SA. Perinatal white matter injury: the changing spectrum of pathology and emerging insights into pathogenetic mechanisms. Ment Retard Dev Disabil Res Rev. 2006; 12(2):129–140. [PubMed: 16807910]
3. Stevenson, DKBW.; Sunshine, P. Fetal and neonatal brain injury: Mechanisms, Management and the Risks of Practice. 3rd Edition. New York: Cambridge University Press; 2003.
4. Hagberg B, G S, Steen M. The disequilibrium syndrome in cerebral palsy. Acta Paediatric Scandinavia (suppl). 1972; 226:1–63.
5. Towfighi J, Mauger D, Vannucci RC, Vannucci SJ. Influence of age on the cerebral lesions in an immature rat model of cerebral hypoxia-ischemia: A light microscopic study. Dev. Brain Res. 1997; 100:149–160. [PubMed: 9205806]
6. Vannucci R, Vannucci SJ. Glucose, acidosis, and perinatal hypoxic-ischemic brain damage. Mental Ment Retard Dev Disabil Res Rev. 1997; 3(1):69–75.
7. Vannucci, RC. Hypoxic-ischemic encephalopathy: Clinical aspects. In: Fanaroff, AA.; Martin, RJ., editors. Neonatal Perinatal Medicine IV. Philadelphia: Mosby-Yearbook, Inc.; 1997. p. 877-891.
8. Vannucci RC, Vannucci SJ. A model of perinatal hypoxic-ischemic brain damage. Ann N Y Acad Sci. 1997 Dec 19.835:234–249. [PubMed: 9616778]

NIH-PA Author Manuscript

NIH-PA Author Manuscript

NIH-PA Author Manuscript

9. Saliba E, Henrot A. Inflammatory mediators and neonatal brain damage. Biol Neonate. 2001; 79(3–4):224–227. [PubMed: 11275656]
10. Stoll G, Jander S, Schroeter M. Inflammation and glial responses in ischemic brain lesions. Prog Neurobiol. 1998 Oct; 56(2):149–171. [PubMed: 9760699]
11. Tan DX, Manchester LC, Sainz R, Mayo JC, Reiter RJ. Antioxidant strategies in protection against neurodegenerative disorders. Expert Opinon on Therapeutic Patents. 2003; 13:1513–1543.
12. Back SA, Han BH, Luo NL, Chricton CA, Xanthoudakis S, Tam J, et al. Selective vulnerability of late oligodendrocyte progenitors to hypoxia-ischemia. J Neurosci. 2002 Jan 15; 22(2):455–463. [PubMed: 11784790]
13. Back SA, Luo NL, Borenstein NS, Volpe JJ, Kinney HC. Arrested oligodendrocyte lineage progression during human cerebral white matter development: dissociation between the timing of progenitor differentiation and myelinogenesis. J Neuropathol Exp Neurol. 2002 Feb; 61(2):197–211. [PubMed: 11853021]
14. Ness JK, Romanko MJ, Rothstein RP, Wood TL, Levison SW. Perinatal hypoxia-ischemia induces apoptotic and excitotoxic death of periventricular white matter oligodendrocyte progenitors. Dev Neurosci. 2001; 23(3):203–208. [PubMed: 11598321]
15. Maurer MH, Tripps WK, Feldmann RE Jr, Kuschinsky W. Expression of vascular endothelial growth factor and its receptors in rat neural stem cells. Neurosci Lett. 2003 Jul 3; 344(3):165–168. [PubMed: 12812831]
16. Jin K, Zhu Y, Sun Y, Mao XO, Xie L, Greenberg DA. Vascular endothelial growth factor (VEGF) stimulates neurogenesis in vitro and in vivo. Proc Natl Acad Sci U S A. 2002 Sep 3; 99(18): 11946–11950. [PubMed: 12181492]
17. Greenberg DA, Jin K. From angiogenesis to neuropathology. Nature. 2005 Dec 15; 438(7070): 954–959. [PubMed: 16355213]
18. Zachary I. Neuroprotective role of vascular endothelial growth factor: signalling mechanisms, biological function, and therapeutic potential. Neurosignals. 2005; 14(5):207–221. [PubMed: 16301836]
19. Galvan V, Greenberg DA, Jin K. The role of vascular endothelial growth factor in neurogenesis in adult brain. Mini Rev Med Chem. 2006 Jun; 6(6):667–669. [PubMed: 16787377]
20. Hashimoto T, Zhang XM, Chen BY, Yang XJ. VEGF activates divergent intracellular signaling components to regulate retinal progenitor cell proliferation and neuronal differentiation. Development. 2006 Jun; 133(11):2201–2210. [PubMed: 16672338]
21. Sun Y, Jin K, Xie L, Childs J, Mao XO, Logvinova A, et al. VEGF-induced neuroprotection, neurogenesis, and angiogenesis after focal cerebral ischemia. J Clin Invest. 2003 Jun; 111(12): 1843–1851. [PubMed: 12813020]
22. Sun Y, Jin K, Childs JT, Xie L, Mao XO, Greenberg DA. Vascular endothelial growth factor-B (VEGFB) stimulates neurogenesis: evidence from knockout mice and growth factor administration. Dev Biol. 2006 Jan 15; 289(2):329–335. [PubMed: 16337622]
23. Zhu Y, Jin K, Mao XO, Greenberg DA. Vascular endothelial growth factor promotes proliferation of cortical neuron precursors by regulating E2F expression. Faseb. J. 2003 Feb; 17(2):186–193. [PubMed: 12554697]
24. Mani N, Khaibullina A, Krum JM, Rosenstein JM. Astrocyte growth effects of vascular endothelial growth factor (VEGF) application to perinatal neocortical explants: receptor mediation and signal transduction pathways. Exp Neurol. 2005 Apr; 192(2):394–406. [PubMed: 15755557]
25. Le Bras B, Barallobre MJ, Homman-Ludiye J, Ny A, Wyns S, Tammela T, et al. VEGF-C is a trophic factor for neural progenitors in the vertebrate embryonic brain. Nat Neurosci. 2006 Mar; 9(3):340–348. [PubMed: 16462734]
26. Rice JE, Vannucci RC, Brierley JB. The influence of immaturity on hypoxic-ischemic brain damage in the rat. Annals of Neurology. 1981; 9:131–141. [PubMed: 7235629]
27. Vannucci RC, Lyons DT, Vasta F. Regional cerebral blood flow during hypoxia-ischemia in immature rats. Stroke. 1988; 19:245–250. [PubMed: 3344541]
28. Vannucci RC, Connor JR, Mauger DT, Palmer C, Smith MB, Towfighi J, et al. Rat model of perinatal hypoxic-ischemic brain damage. J Neurosci Res. 1999; 55(2):158–163. [PubMed: 9972818]

NIH-PA Author Manuscript

NIH-PA Author Manuscript

NIH-PA Author Manuscript

29. Young G, Levison S. An improved method for propagating oligodendrocyte progenitors in vitro. J Neurosci Methods. 1997; 77:163–168. [PubMed: 9489893]
30. Levison, S.; McCarthy, K. Astroglia in Culture. In: Banker, G.; Goslin, K., editors. Culturing Nerve Cells. Cambridge: MIT press; 1991. p. 309-336.
31. Ness JK, Mitchell NE, Wood TL. IGF-I and NT-3 signaling pathways in developing oligodendrocytes: differential regulation and activation of receptors and the downstream effector Akt. Developmental Neuroscience. 2002; 24(5):437–445. [PubMed: 12666655]
32. Tavazoie M, Van der Veken L, Silva-Vargas V, Louissaint M, Colonna L, Zaidi B, et al. A specialized vascular niche for adult neural stem cells. Cell Stem Cell. 2008 Sep 11; 3(3):279–288. [PubMed: 18786415]
33. Shen Q, Wang Y, Kokovay E, Lin G, Chuang SM, Goderie SK, et al. Adult SVZ stem cells lie in a vascular niche: a quantitative analysis of niche cell-cell interactions. Cell Stem Cell. 2008 Sep 11; 3(3):289–300. [PubMed: 18786416]
34. Currle DS, Gilbertson RJ. The niche revealed. Cell Stem Cell. 2008 Sep 11; 3(3):234–236. [PubMed: 18786409]
35. Mirzadeh Z, Merkle FT, Soriano-Navarro M, Garcia-Verdugo JM, Alvarez-Buylla A. Neural stem cells confer unique pinwheel architecture to the ventricular surface in neurogenic regions of the adult brain. Cell Stem Cell. 2008 Sep 11; 3(3):265–278. [PubMed: 18786414]
36. Wada T, Haigh JJ, Ema M, Hitoshi S, Chaddah R, Rossant J, et al. Vascular endothelial growth factor directly inhibits primitive neural stem cell survival but promotes definitive neural stem cell survival. J Neurosci. 2006 Jun 21; 26(25):6803–6812. [PubMed: 16793887]
37. Schanzer A, Wachs FP, Wilhelm D, Acker T, Cooper-Kuhn C, Beck H, et al. Direct stimulation of adult neural stem cells in vitro and neurogenesis in vivo by vascular endothelial growth factor. Brain Pathol. 2004 Jul; 14(3):237–248. [PubMed: 15446578]
38. Krum JM, Rosenstein JM. VEGF mRNA and its receptor flt-1 are expressed in reactive astrocytes following neural grafting and tumor cell implantation in the adult CNS. Experimental Neurology. 1998 Nov; 154(1):57–65. [PubMed: 9875268]
39. Krum JM, Mani N, Rosenstein JM. Angiogenic and astroglial responses to vascular endothelial growth factor administration in adult rat brain. Neuroscience. 2002; 110(4):589–604. [PubMed: 11934468]
40. Krum JM, Mani N, Rosenstein JM. Roles of the endogenous VEGF receptors flt-1 and flk-1 in astroglial and vascular remodeling after brain injury. Exp Neurol. 2008 Jul; 212(1):108–117. [PubMed: 18482723]
41. Arai Y, Deguchi K, Takashima S. Vascular endothelial growth factor in brains with periventricular leukomalacia. Pediatr Neurol. 1998 Jul; 19(1):45–49. [PubMed: 9682885]
42. Moreno-Lopez B, Romero-Grimaldi C, Noval JA, Murillo-Carretero M, Matarredona ER, Estrada C. Nitric oxide is a physiological inhibitor of neurogenesis in the adult mouse subventricular zone and olfactory bulb. J Neurosci. 2004 Jan 7; 24(1):85–95. [PubMed: 14715941]
43. Matarredona ER, Murillo-Carretero M, Moreno-Lopez B, Estrada C. Nitric oxide synthesis inhibition increases proliferation of neural precursors isolated from the postnatal mouse subventricular zone. Brain Res. 2004 Jan 9; 995(2):274–284. [PubMed: 14672818]
44. Massaro AR, Sbriccoli A, Tonali P. Reactive astrocytes within the acute plaques of multiple sclerosis are PSA-NCAM positive. Neurol Sci. 2002 Dec; 23(5):255–256. [PubMed: 12528689]
45. Hirayama A, Okoshi Y, Hachiya Y, Ozawa Y, Ito M, Kida Y, et al. Early immunohistochemical detection of axonal damage and glial activation in extremely immature brains with periventricular leukomalacia. Clin Neuropathol. 2001 Mar-Apr;20(2):87–91. [PubMed: 11327303]
46. Sizonenko SV, Camm EJ, Dayer A, Kiss JZ. Glial responses to neonatal hypoxic-ischemic injury in the rat cerebral cortex. Int J Dev Neurosci. 2008 Feb; 26(1):37–45. [PubMed: 17942266]
47. Kinney, HC.; Armstrong, DD. Perinatal Neuropathology. In: Graham, DI.; Lantos, PL., editors. Greenfield's Neuropathology. New York: Oxford; 2002. p. 519-606.
48. Shin YJ, Choi JS, Choi JY, Cha JH, Chun MH, Lee MY. Enhanced expression of vascular endothelial growth factor receptor-3 in the subventricular zone of stroke-lesioned rats. Neurosci Lett. 2010 Jan 22; 469(2):194–198. [PubMed: 19963036]

NIH-PA Author Manuscript

NIH-PA Author Manuscript

NIH-PA Author Manuscript

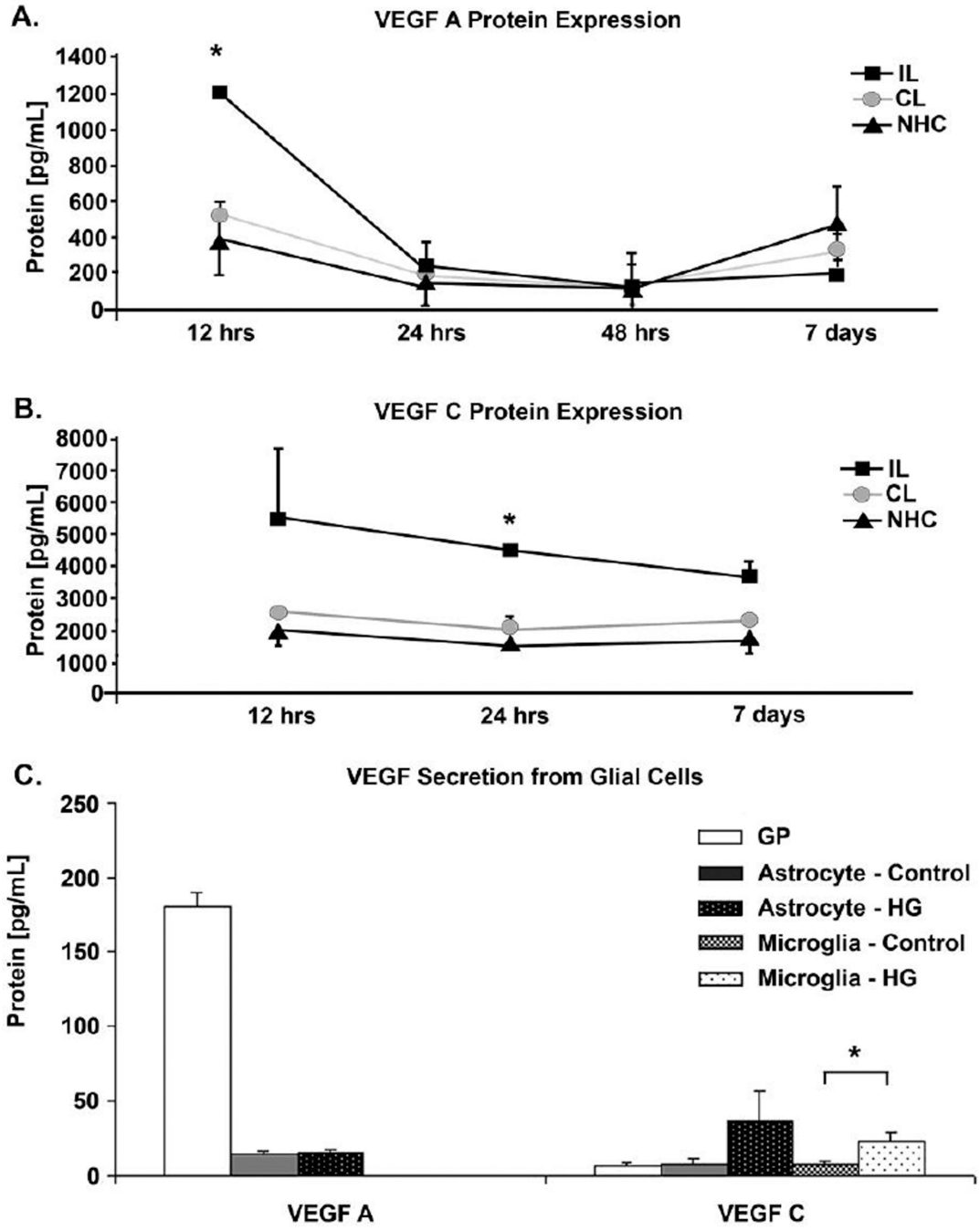

Figure 1. VEGF-A and C protein expression

A, B. ELISAs were performed for VEGF-A (A) and VEGF-C (B) on protein samples isolated from microdissected SVZs (subventricular zones) at time points varying from 12 h – 7 d after neonatal H-I (hypoxia-ischemia) (n=4 per sample). Error bars = SEM. * denotes $p < 0.05$ using student's t-test between IL (ipsilateral) and both CL (contralateral) and NHC (non-hypoxic control) hemisphere protein samples. C. ELISAs were performed on supernatants from glial progenitor spheroids (GP), astrocytes and microglia. Spheroids were continuously grown in 2% oxygen and astrocytes and microglia were exposed to 2% oxygen and glucopenic conditions for 2 h (hypoxic-glucopenic, HG). Media was collected 24 h after returning the cells to atmospheric, normoglycemic (control) conditions, n=4 for each

condition. Error bars = SEM. * denotes significant t-test ($p < 0.05$) between control and HG conditions for each cell type.

NIH-PA Author Manuscript
NIH-PA Author Manuscript
NIH-PA Author Manuscript

NIH-PA Author Manuscript
NIH-PA Author Manuscript
NIH-PA Author Manuscript

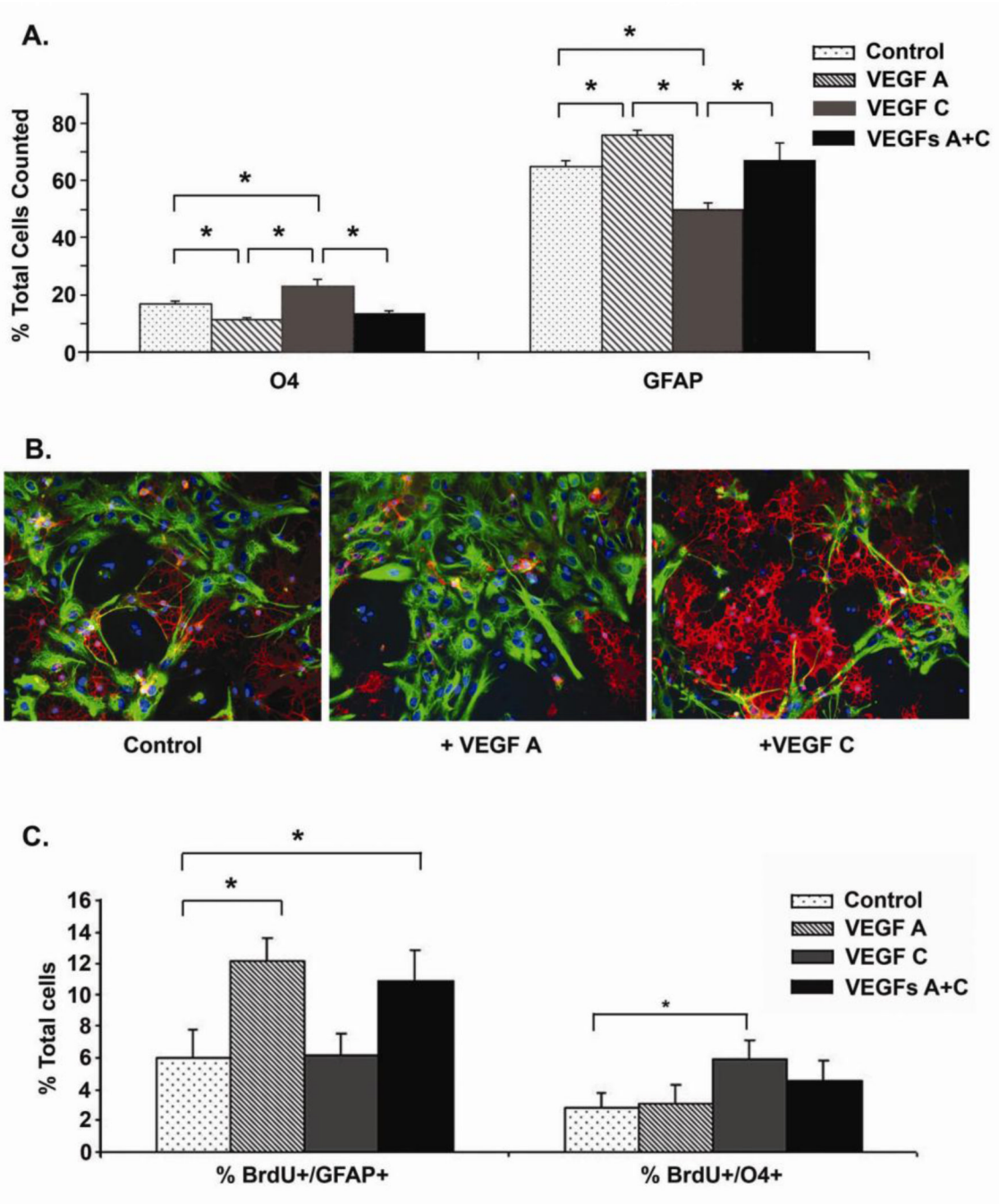

Figure 2. VEGFs A and C differentially affect glial generation from spheroids in vitro

Spheroids were gently dissociated into single cells and plated for 6 h prior to the addition of growth factors for 96 h. A–B, Representative image of cells maintained in N2B2, VEGF-A and VEGF-C and stained for O4 (red), GFAP (green) and DAPI (blue) in B. Graphs depict averaged data from counting at least 100 cells from 4 wells for each treatment. Error bars = SEM. * denotes $p < 0.05$ compared to control conditions using student's t test. E. BrdU (10 μM) was added to the media during the last 4 h of incubation with growth factors. Cells were stained for O4, GFAP, BrdU and DAPI (C). Graphs depict averaged data from counting at least 100 cells from 4 wells for each treatment. Data are representative of 2–3

independent experiments. Error bars = SEM. * denotes $p < 0.05$ ANOVA with Fisher's PLSD post-hoc test.

NIH-PA Author Manuscript
NIH-PA Author Manuscript
NIH-PA Author Manuscript

NIH-PA Author Manuscript
NIH-PA Author Manuscript
NIH-PA Author Manuscript

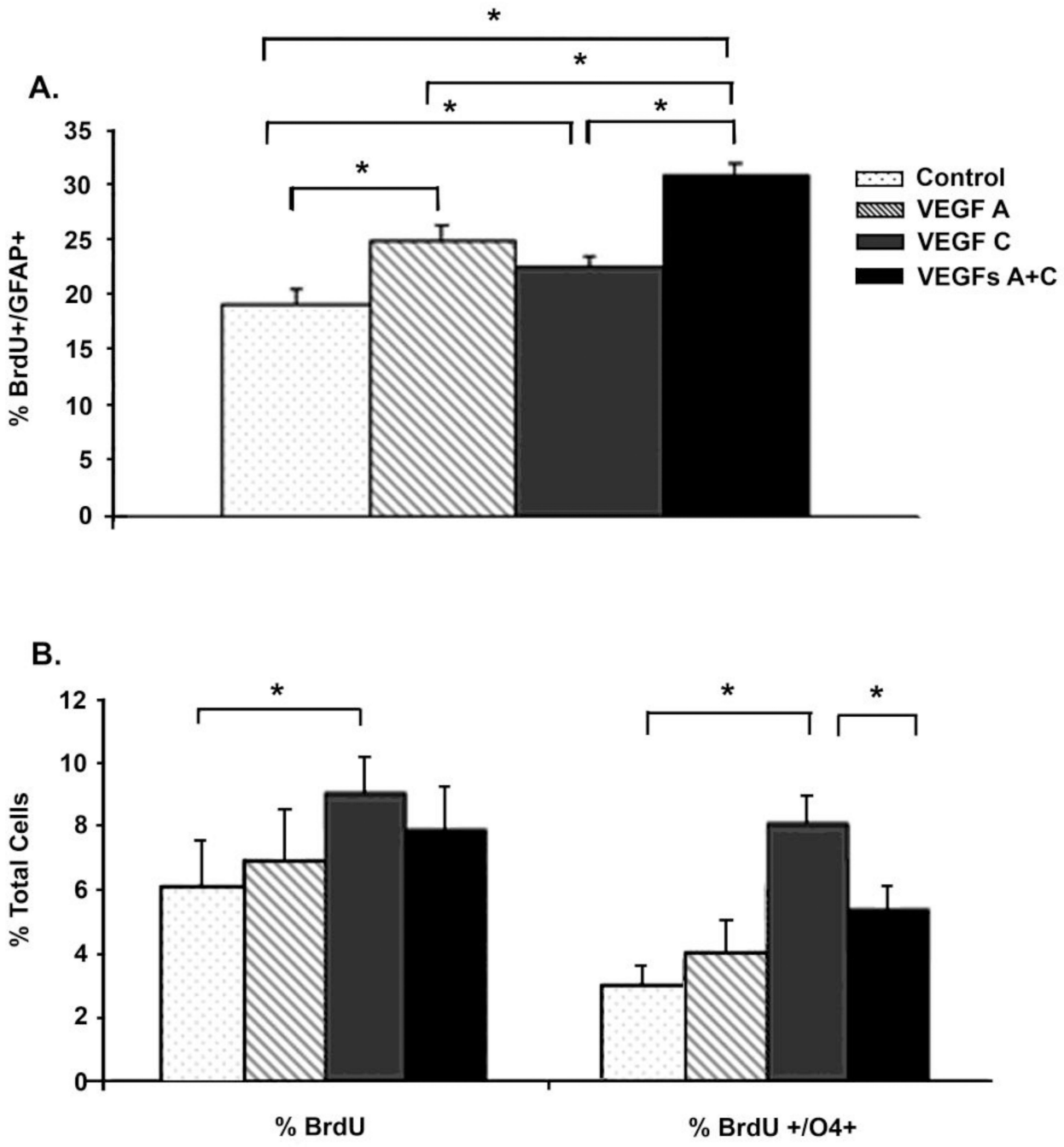

Figure 3. VEGF-A and C cooperate to stimulate astrocyte proliferation but only VEGF-C alone stimulates oligodendrocyte progenitor proliferation

A) Astrocytes from neonatal mixed glial cultures were plated onto chamber slides overnight in N2B2 alone or supplemented with 8 ng/mL VEGF-A and/or 100 ng/mL VEGF-C. After 18 h BrdU was added and 2 hours later the cells were fixed and stained for BrdU, GFAP and DAPI. B) Oligodendrocyte progenitor cells (OPCs) were generated from mixed glial cultures and plated onto chamber slides overnight in N2B2 with 0.5% serum, followed by a 6 h starvation period. Then media was supplemented with 8 ng/mL VEGF-A and/or 100 ng/mL VEGF-C and 10uM BrdU was added during the final 2 h of an 18 h treatment. Chamber slides were fixed and stained for BrdU, O4 and DAPI. Graphs represent averaged data from

counting at least 100 cells from 4 wells for each treatment. Data are representative of 2–3 independent experiments. Error bars = SEM. * denotes $p < 0.05$ compared to control conditions using ANOVA analysis with Fisher's post-hoc test.

NIH-PA Author Manuscript
NIH-PA Author Manuscript
NIH-PA Author Manuscript

NIH-PA Author Manuscript
NIH-PA Author Manuscript
NIH-PA Author Manuscript

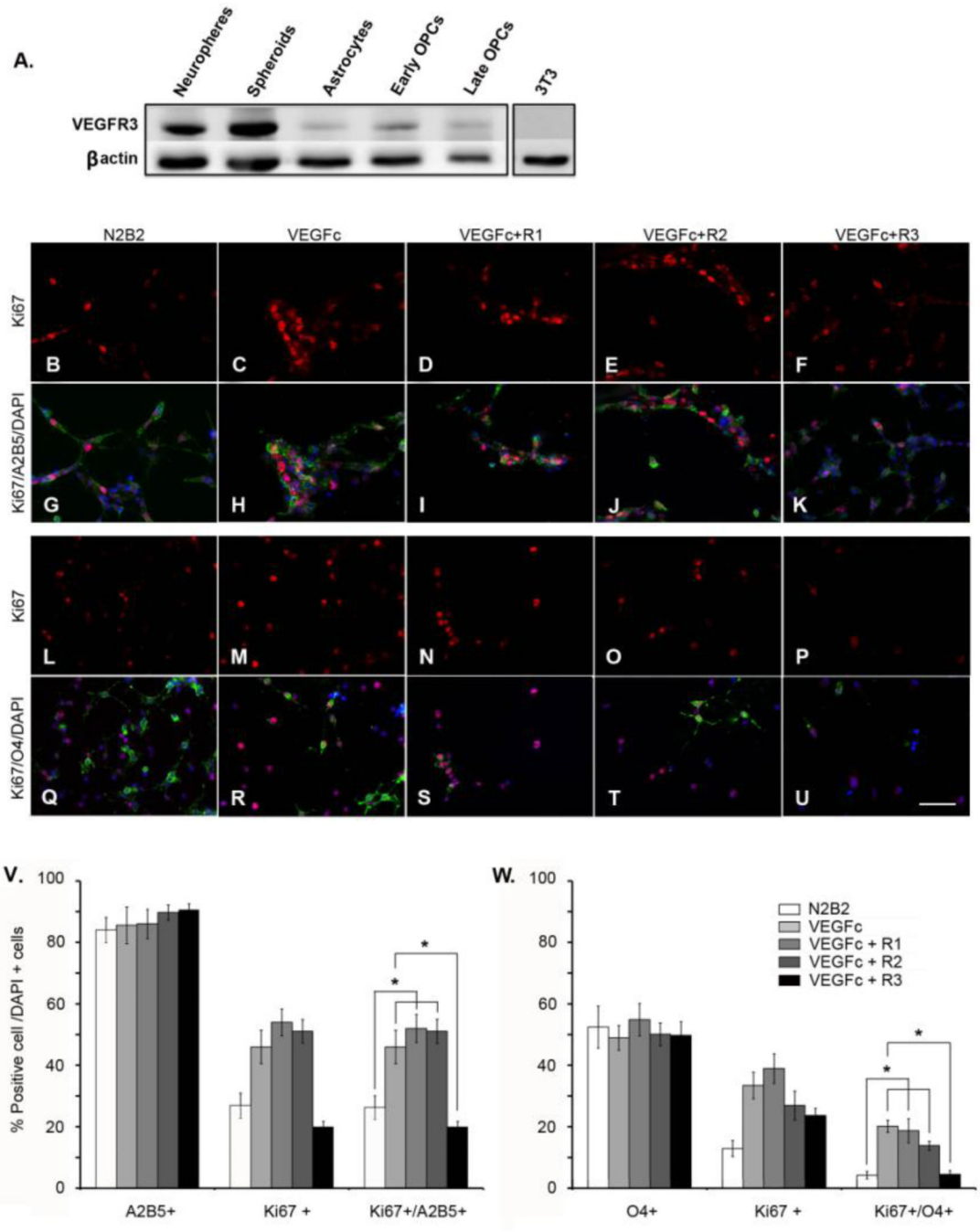

Figure 4. VEGFR-3 is expressed by neural precursors and blocking VEGFR-3, but not VEGFR-1 or R2, abolishes VEGF-C stimulated oligodendrocyte proliferation

A. Neurospheres and spheroids were generated from neonatal rat SVZs and cultured for 7 DIV in 2%O_2, 5% CO_2, 93% N_2. Astrocytes and oligodendrocyte progenitor cells (OPCs) were generated from mixed glial cell cultures from neonatal rat brains. Fibroblasts (3T3) were grown in 10% serum containing medium. Expression of VEGFR-3 (Flt4) (175kDa) was evaluated by Western Blot. Data are representative of 3 independent experiments. B–U. Early OPCs were incubated with either VEGF-C (100ng/ml) or neutralizing antibodies to VEGFR-1 (5μg/ml), VEGFR-2 (0.2μg/ml) or VEGFR-3 (7.5μg/ml) in N2B2 medium. Cells were double immunostained for Ki67 with either A2B5 or O4 and counterstained with

NIH-PA Author Manuscript

NIH-PA Author Manuscript

NIH-PA Author Manuscript

DAPI, (B–U). VEGF-C promoted proliferation of both early OPCs (C,H) and also late OPCs (M,R), compared with N2B2 control medium (B,G,L,Q). The neutralizing antibody to VEGFR-3 completely blocked VEGF-C-stimulated OPC proliferation (F, K, P, U). In contrast, neutralizing antibodies to VEGFR-1 or R2 did not inhibit VEGF-C function (D, I, N, S; and E, J, M, T). Scale bar represents 50 μM.

V+W. Quantification of both A2B5+ (V), and O4+ OPCs (W), *P<0.05 by ANOVA followed by X post-hoc test.

NIH-PA Author Manuscript

NIH-PA Author Manuscript

NIH-PA Author Manuscript

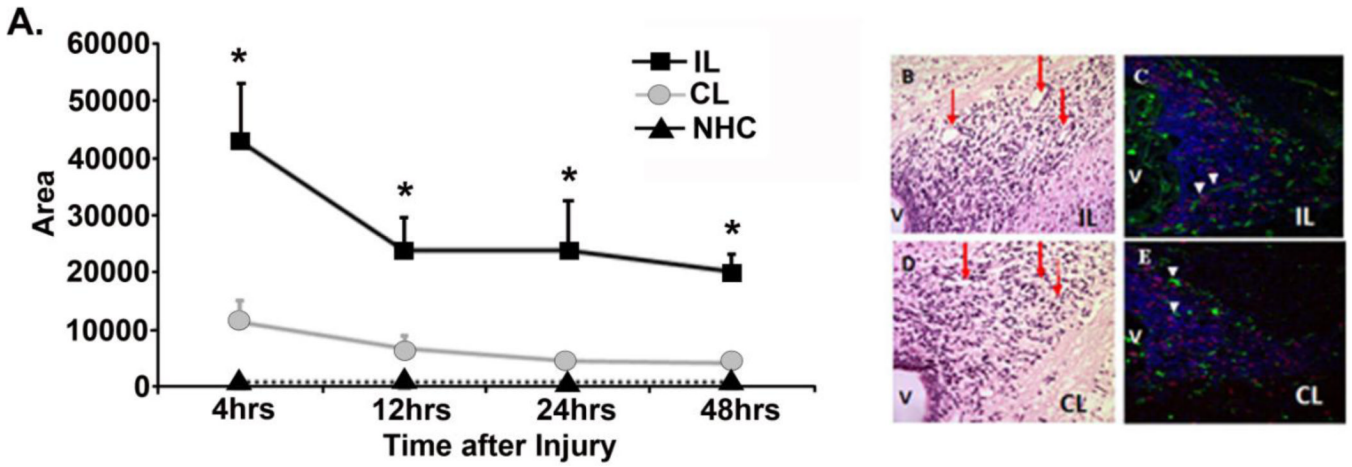

Figure 5. Microvasculature changes in SVZ after neonatal H-I

Paraffin-embedded sections spanning 4 to 48 h of recovery from H-I were stained with hematoxylin and eosin and blood vessels were identified by morphology (red arrows) in IL (B) and CL (D) hemispheres (D). Morphometric analysis was performed on 40X images of corresponding vessels in the SVZ using IP Lab (Scanalytics, Inc. Fairfax, Virginia USA). Sections from 4h brains were stained for BrdU (red), tomato lectin (green) and DAPI (blue) to label proliferating blood vessels (white arrowheads) in IL (C) and CL hemispheres (E). IL = ipsilateral hemisphere, CL = contralateral hemisphere, NHC = non-hypoxic control. N = 8 vessels measured from 3 random, nonadjacent SVZ sections and 4 animals at each time point. Error bars = SEM. * indicates $p < 0.05$ compared to both CL and NHC. (V = ventricles)

NIH-PA Author Manuscript

NIH-PA Author Manuscript

NIH-PA Author Manuscript

Table 1

Primers used for Sybr Green Quantitative Real Time - PCR

Growth Factor	Specific Primer Sequences	PCR Product Size
VEGF – A	Forward: 5'- GGG CTG GTG CAA TGA TGA AG – 3' Reverse: 5'- GTG AGG TTT GAT CCG CAT GA – 3'	84bp
VEGF – B	Forward: 5'- GTG GCT GCT GTC CTG ACG AT -3' Reverse: 5'- TGC TCG GGT ACT GGA TCA TG -3'	90bp
VEGF – C	Forward: 5'- TCA GCA AGA CGT TGT TTG AAA TTA -3' Reverse: 5'- CAG GAA TGA TTG GCA AAA CT -3'	85bp